Scaling effects in Schottky contacts

A. Ruzin
School of EE, Faculty of Engineering, Tel Aviv University, 69978 Tel Aviv, Israel

(Received 4 August 2015; accepted 31 October 2015; published online 23 November 2015)

This article reports on scaling effects in Schottky contacts on various types of semiconductors, including low resistivity, semi-intrinsic, and deep-level compensated. The investigation was performed using a finite element computation and drift-diffusion transport model. In low resistivity semiconductors, the currents scale with contact area as long as thermionic emission process dominates the current transport, with limited impact of velocity saturation effect. In high resistivity semiconductors, the scaling is much more complex due to the considerable impact of minority carrier contribution. In several cases, the currents scale with contact radius, rather than with area, due to corresponding electric field variations. In some compensated materials, the impact of velocity saturation was shown to boost the current, due to carrier accumulation and corresponding space charge variations. © *2015 AIP Publishing LLC*. [http://dx.doi.org/10.1063/1.4935628]

I. INTRODUCTION

As technology progresses, the electronic devices' dimensions keep decreasing, improving circuits' performance (power consumption, bandwidth, etc.). One of the side effects of this global device down-scaling is the corresponding down-scaling of the contacts (both ohmic and Schottky). Another important field of variable contact dimensions is that of detectors, where the contact size corresponds to that of the desirable pixel, and does not necessarily reflect the technological limits. Such pixels dimensions typically range from millimeters (e.g., x-ray imaging) to microns (e.g., digital cameras). It is well known that in finite contacts the electric field (E-field) lines are denser near the contact edges than at the central region. Most effects related to this non-uniformity are usually classified as "edge-effects." *In addition* to this E-field non-uniformity over the contact area, the depth profile of E-field at the contact center depends on the contact size. Since, the current density is often related to E-field intensity; it potentially becomes contact size dependent, and non-uniform underneath the contact. In addition to its contribution to drift current, the high local E-field may enhance breakdown, Poole-Frenkel effect, etc. The "scaling" of contacts usually refers to the dependence of I-V curves on the contact dimensions (usually area); thus, linear scaling most likely indicates current density (J) independence on the contact size. The wider and more comprehensive analysis of contact down scaling is particularly important when high voltage is to be applied, as in the case of gamma-ray (or particle) detector. This study addresses various aspects of Schottky contact downscaling, and emphasizes the challenging application of Schottky contacts for detector devices ($Cd_{1-x}Zn_xTe$, Si(Li), SiGe(Li), etc.).

One of the more challenging operation modes for particle detectors is spectroscopy. Given the atomic number and thickness requirements were respected to yield sufficient detection efficiency, in order to obtain high energy resolution the high charge collection efficiency must be combined with low electronic noise.

DC Current: Low frequency noise mechanisms, such as 1/f, are known to be proportional to a power of the DC current (I^{α}). In junction based devices the "white," shot-noise mechanism is also proportional to a power of the DC current.

In junction based devices (e.g., Schottky barriers) operated under reverse bias conditions, the origin and magnitude of dark current is not straightforward. The classic "textbook" approach attributes the current to thermionic emission of the free *majority* carriers over the Schottky barrier (e.g., for n-type semiconductors, electrons emitted from the metal contact)[1,2]

$$J_e = A^* T^2 \exp\left(\frac{-q\phi_B}{k_B T}\right)\left[\exp\left(\frac{qV}{k_B T}\right) - 1\right]; \quad A^* = \frac{qm^* k_B^2}{2\pi^2\hbar^3}, \tag{1}$$

where A^* is the effective Richardson constant, T is temperature in Kelvin, k_B is the Boltzmann constant, ϕ_B is the Schottky barrier height, q is electron charge, $\hbar$ is the reduced Planck constant, and m^* is the effective mass of the majority carriers. Additional current component due to generation in the depletion region can be straightforwardly accounted for. However, this is only a fair approximation in the case of highly extrinsic semiconductors, where the Schottky interface concentration of the minority carriers is negligible, and the resistivity of the neutral bulk is low. In semi-intrinsic (SI or REF) Schottky devices with high potential barriers (e.g., $Cd_{1-x}Zn_xTe$, $Si_{1-x}Ge_x$(Li)), the conductivity by minority carriers may be higher by far compared to the thermionic emission current. In addition, it was shown that in such devices hole injection may take place.[3,4] The electron and hole current densities at the Schottky contact interface should be described as

$$\begin{aligned} J_e \cdot \vec{n} &= q v_{TE,e}([e]^S - [e]^S_{TDE}), \\ J_h \cdot \vec{n} &= q v_{TE,h}([h]^S - [h]^S_{TDE}), \end{aligned} \tag{2}$$

where $\vec{n}$ is a unit vector normal to the contact interface, $[e]^S_{TDE}$, $[h]^S_{TDE}$ represent the thermo-dynamic equilibrium interface concentrations of electrons and holes, respectively, and $[e]^S$, $[h]^S$ represent those concentrations under bias. The

thermionic emission velocities (sometimes called Schottky recombination or Richardson velocities), $v_{TE,e,h}$, are defined in Ref. 5 as

$$v_{TE,e,h} = \sqrt{\frac{k_B T}{2\pi m^*_{e,h}}}, \tag{3}$$

where $m^*_{e,h}$ are the effective masses of electron and hole, respectively. The solution of the Schottky contact currents by the set of Eq. (2) is much more precise than the commonly used text book approximation of Eq. (1). Beside the inclusion of the minority carrier contribution, numerical solution of equation set (2) accounts for the quasi-Fermi levels of the carriers at the interface, while Eq. (1) assumes validity of Fermi level even under bias. It can be readily shown that the current component of the *majority* carriers of equations set Eq. (2) is equivalent to Eq. (1), under the above mentioned approximation. The thermionic emission approximation described by Eq. (1) has an "interfacial layer-thermionic-diffusion theory" extension by Wu.[6] It accounts for majority carriers only, assumes a presence of an interface insulating barrier layer, and includes numerous fitting parameters. In some cases, the "Wu model" has been shown to fit *reverse* currents of Pt-CdZnTe-Pt MSM structures in a wide bias range.[7]

Schottky devices on high resistivity semiconductors are not expected to yield as low reverse currents as majority thermionic emission (Eq. (1)), but it may still be lower compared to the conduction by majority carriers in ohmic-like MSM devices.

Active region: The thick active region required for high absorption efficiency also yields low device capacitance, required for low electronic noise. In extrinsic, low-ρ, semiconductors (with a valid depletion approximation) the depletion layer width under a junction is roughly proportional to $\sqrt{V_D/N_x}$ (N_x being the dominant doping concentration and V_D the reverse bias). Thus, in this case the "full depletion bias" (required for maximum active volume and minimum device capacitance) could be very high, raising reliability, and safety questions. In SI, *uncompensated*, semiconductors the junction built-in potential or low externally applied reverse bias may fully deplete the device of majority carriers.[3,4] Therefore, maximal active thickness and minimal device capacitance do not require extreme biasing conditions (similar to the ohmic-like devices). In *deep-level compensated*, semi-insulating semiconductors the active layer is determined by the cross-sections of the compensating deep-levels, as shown in Section III.

This study compares the scaling effects in Schottky contact on low resistivity (extrinsic) semiconductors and on various high resistivity semiconductors, including semi-intrinsic and deep-level compensated. Particular emphasis is made on the deep-level compensated material since it is the least studied instance. This case is also of particular importance in wide band-gap materials (e.g., II-VI group), and highly irradiated semiconductors. For instance, silicon based detectors after exposure to moderate fluences of minimum ionizing particles (MIP), exhibit compensated behavior. In this study, the calculations were performed for a single crystal $Cd_{1-x}Zn_xTe$ ternary alloy. However, the conclusions are valid with appropriate adjustments to other semiconductors as well. The current conduction model used for these generic calculations is drift-diffusion.

In spite of the considerable amount of research conducted with $Cd_{1-x}Zn_xTe$ and other wide bandgap II-VI group semiconductors, the mechanism responsible for high resistivity remains vague. The binary and ternary alloys of the $Cd_{1-x}Zn_xTe$ family are grown by a variety of methods.[8–10] For each growth method, the growth conditions vary in each recipe, in particular, the ratio of cadmium-telluride during the growth. In addition it is a common practice introducing doping elements in the growth process (e.g., indium as a shallow level donor and germanium as a deeper level donor), and finalizing the material preparation by a tailored annealing procedure.[11,12] Given the high defect density observed in these alloys, and the fact that even moderate thermal treatment (>300 °C) can modify its resistivity, it is generally accepted that the high resistivity is the result of a compensation process.

Previous experimental observations show that the currents in Schottky contacts of nano-scale dimensions often do not scale (linearly) with area or with perimeter. Furthermore, some experimental results indicate *current density* reduction.[13,14] while others show the opposite effect.[15] There are considerable analytical as well as numerical modeling efforts; however, these are mostly two-dimensional calculations, often based on classical approximations (such as the depletion approximation), not accounting for velocity saturation, free carrier charge, etc.[14,16–19] Most published results refer to low resistivity semiconductors that are more common in the microelectronics industry. The issue of contacts in general and contact scaling, in particular, to *high resistivity semiconductors*, such as $Cd_{1-x}Zn_xTe$, received less attention, and needs to be addressed. It has been recently demonstrated that the energy band diagram structure under "infinite" contacts on high-ρ semiconductor is very different from that of the low-ρ case, for both, uncompensated and compensated semiconductors.[3,4] It was theoretically shown that ohmic contacts on *non-compensated* semiconductor yield Schottky-like potential barriers when downscaled to nano-meter size.[20] The experimental results of indium nano-contacts on high-resistivity, n-type $Cd_{1-x}Zn_xTe$ (with $E_g = 1.6$ eV corresponding to $x \approx 0.15$–0.2) seem to concur with these calculations.[21] The dimension range of particular interest for detector application does not reach deep into sub-micron, thus this work emphasizes the cm-μm range.

II. "EXPERIMENTAL" APPROACH AND METHODOLOGY

In this study, three-dimensional finite-element computer simulation program was used to solve combined Poisson and continuity equations of electrons and holes in semiconductor devices.[22] In order to allow straightforward comparison of low and high resistivity materials, all calculations were performed using one semiconductor: n-type $Cd_{1-x}Zn_xTe$ single crystal bulk material with $E_{gap} = 1.6$ eV, corresponding to $x \approx 0.15$ (for convenience it will be referred as $Cd_{0.85}Zn_{0.15}Te$). The effective masses in CdTe–$Cd_{1-x}Zn_xTe$

for both, density of state (DOS), and for conductivity were investigated since the 1960s.[23–26] In this work, commonly used values of $m_e^* = 0.0963 m_0$ and $m_h^* = 0.37 m_0$ were adopted.[27] These values yield thermionic emission velocities of $v_{TE,e} \approx 8.6 \times 10^6$ cm/s and of $v_{TE,h} \approx 4.5 \times 10^6$ cm/s, and Richardson constant, A^*, for electron current ~12 (A/cm^2/K^2). However, it should be noted that this study is of generic nature and the exact values are not critical. Schottky contacts were defined with 1.0 eV barriers (as the *actual barrier*, accounting for all: work-functions, electron affinity, surface states, etc.).

In spectroscopy grade $Cd_{0.85}Zn_{0.15}Te$ devices, the reported resistivity is in the range of 10^8–10^{11} Ωcm. In this study, a value of $\sim 10^{10}$ Ωcm was selected, for the high resistivity case. For mobilities of $\mu_e = 1000$ and $\mu_h = 80$ (cm^2 V^{-1} s^{-1}), resistivity of 10^{10} Ωcm corresponds to free electron concentration of $[e] \sim 6.13 \times 10^5$ cm^{-3} (nearly an order of magnitude above the intrinsic concentration). Thus, the material can be referred as weak n-type (or ν-type). For the low resistivity, extrinsic "textbook" case shallow donors $N_D = 10^{16}$ cm^{-3} were defined at energy level E_C–0.05 eV (fully ionized at 300 K).

Table I summarizes the six investigated material cases (one low resistivity and five high resistivity options). It is important to stress that all five high resistivity material yield $\sim 10^{10}$ Ωcm resistivity at thermo-dynamic equilibrium (TDE). All four deep-donor compensated semiconductors assume shallow acceptor concentration of 10^{16} cm^{-3}, and deep donor concentration of 5×10^{18} cm^{-3} (at energy level $E_{DD} = E_V + 0.72$ eV). The four cases of deep donor compensation discussed *differ only in capture cross-sections of electrons and holes*: equal-low cross-sections (LL), equal-high cross-sections (HH), electron-trap cross-sections (HL), and hole-trap cross-sections (LH).

The $Cd_{0.85}Zn_{0.15}Te$ bulk has a disk shape with 500 μm thickness and 2 cm radius. On the back side of the bulk a full size, ideal ohmic contact was defined. On the front side cylindrical Schottky contacts were set, with radii, $r_C = 10$ nm–20 mm; where $r_c = 20$ mm is a "full size contact"—corresponding to an infinite contact case.

The combination of high reverse bias, required for detector operation, and contact downscaling is expected to yield very high local electric field (E-field). It is well known that at high electric fields the velocities of the free carriers in semiconductors saturate, and no longer follow the linear $v = \mu E$ relation. Very little is known about the mobility dependence on E-field in $Cd_{1-x}Zn_xTe$ semiconductor family. Numerous authors report linear Electric field-velocity dependence (indicating constant mobility) in the *detector operation bias range*. However, at higher E-fields it has been reported that free electrons in CdTe have a negative differential mobility.[28,29] To explain this behavior, a hypothesis was suggested that electrons, heated by the electric field, transfer into an energetically higher side valley with a much larger effective mass.[30] The model based on this well established hypothesis is called transferred electron model can be expressed in terms of electron velocity or mobility dependence[31]

$$v = \frac{\mu_0 E + v_{Sat}(E/E_0)^\beta}{1 + (E/E_0)^\beta}; \quad or \quad \mu = \frac{\mu_0 + (v_{Sat}/E)(E/E_0)^\beta}{1 + (E/E_0)^\beta}, \tag{4}$$

where μ_0 is the low field mobility, v_{Sat} is the saturation velocity (after the peak), E_0 is the electric field corresponding to the velocity peak, β is a parameter, and E is the actual E-field. Fair fit for the CdTe experimental results is achieved with a set ($\beta = 4$, $v_{Sat} = 10^7$, $E_0 = 15\,000$, and $\mu_0 = 1000$) applied to electron mobility. Even less information exists in the literature regarding hole velocity saturation and hole mobility dependence on E-field. It has been reported by Ottaviani *et al.*[32] that hole mobility in CdTe *increases* with E-field (up to ~50 kV/cm). The increase is more pronounced at low temperature and practically negligible at 300 K, which is consistent with Poole-Frenkel effect.

A very common analytical treatment of mobility is the one proposed in 1967 for silicon by Caughey and Thomas[33] and later adopted and confirmed by Canali *et al.*[34]

$$\mu(E) = \mu_0 \left[1 + \left(\frac{\mu_0 E}{v_{Sat}}\right)^\beta\right]^{-\frac{1}{\beta}}. \tag{5}$$

Both models describe velocity saturation effect, thus for a generic study, describing principle effects the model selection is not critical. The later model yields higher calculation speed and better convergence (compared to the transferred electron model), while producing rather similar electron mobility dependence for $\beta \geq 2$. Therefore, in this work we assume Caughey and Thomas (or Canali) model with velocity saturation of 10^7 cm/s for both, electrons and holes (common value range for most semiconductors). The values of $\beta_{e,h} = 2$ taken for $Cd_{0.85}Zn_{0.15}Te$ imply that the mobilities *start* decreasing at E-fields of a few kV/cm.

This article concentrates on the impact of downscaling on classical drift-diffusion current model. For *deep* sub-micron contacts additional current mechanisms may play a role, such

TABLE I. Summary of deep and shallow levels in the simulated material types.

Set	N_D @ ($E_C - 0.02$ eV) shallow donor	N_A @ ($E_V + 0.15$ eV) shallow acceptor	N_{DD} @ ($E_V + 0.72$ eV) deep donor σ_e, σ_h in (cm^2)
REF	6.2×10^5 cm^{-3}	0	0
Low-ρ	1×10^{16} cm^{-3}	0	0
HH	…	1×10^{16} cm^{-3}	5×10^{18} cm^{-3} ($\sigma_e = 10^{-14}$; $\sigma_h = 10^{-14}$)
HL	…	1×10^{16} cm^{-3}	5×10^{18} cm^{-3} ($\sigma_e = 10^{-14}$; $\sigma_h = 10^{-20}$)
LH		1×10^{16} cm^{-3}	5×10^{18} cm^{-3} ($\sigma_e = 10^{-20}$; $\sigma_h = 10^{-14}$)
LL	…	1×10^{16} cm^{-3}	5×10^{18} cm^{-3} ($\sigma_e = 10^{-20}$; $\sigma_h = 10^{-20}$)

as non-local tunneling, and also mobility overshoot may occur due to ballistic transport. In such cases, the classical drift-diffusion approach may not concur with the experimental result, and hydrodynamic (energy balance) models are required. These additional nano scale effects are very case dependent and the experimentally deduced model parameters greatly affect the calculated results. Introduction of such models may be useful for explanation of specific experimental results; however, in this "generic approach" article it would miss the goal.

III. CALCULATED RESULTS AND DISCUSSION

A. Infinite contacts at TDE

In principle, the Green function for planar infinite geometry is well known and the analytical solution of Eq. (6) can be applied

$$-\nabla^2\varphi = \frac{\rho}{\varepsilon}, \tag{6}$$

where ρ is the space charge density, ε is the permittivity, and φ is the potential. However, the space charge distribution has to be known (or assumed), which is not straightforward in high resistivity semiconductors. For the uncompensated, SI semiconductors the space charge density of the dopant atoms is very low (in our case approximately $6 \times 10^5\,\mathrm{cm}^{-3}$); thus, the space charge contribution of the free minority carriers under the Schottky contact becomes dominant. Since the free *hole* density is dominant and it varies with the depth, the total space charge density is far from constant and the concept of "depletion region" approximation cannot be used; obviously, the potential depth profile is no longer parabolic as in the textbook case based on the constant space charge density in the depletion region. Since the device thickness is limited and the overall space charge density (of the ionized donors and the free carriers) is low, the device may be "fully depleted" of majority carriers even at zero external bias. This implies non-zero constant E-field component in the first integration of Eq. (6). The resulting energy band diagrams at TDE are shown in Fig. 1 for Schottky barriers of 1 eV, 1.1 eV, and 1.2 eV on uncompensated (REF) 500 μm thick bulk with donor density of $6.02 \times 10^5\,\mathrm{cm}^{-3}$. The corresponding hole interface concentrations, $[h]^S_{TDE}$, are approximately 6×10^8, 3×10^{10}, 1×10^{12} cm^{-3}, respectively. Up to barrier height of ~1.1 eV, the TDE energy bands exhibit negligible bending, indicating *nearly uniform* E-field solution (implying insignificant space charge density). In fact in the REF semiconductor, the space charge of the ionized donors does not cause noticeable band bending *in the bulk*, and only the charge of the free holes may yield a noticeable band bending near the interface (for $\Phi_B > 1.1$ eV).

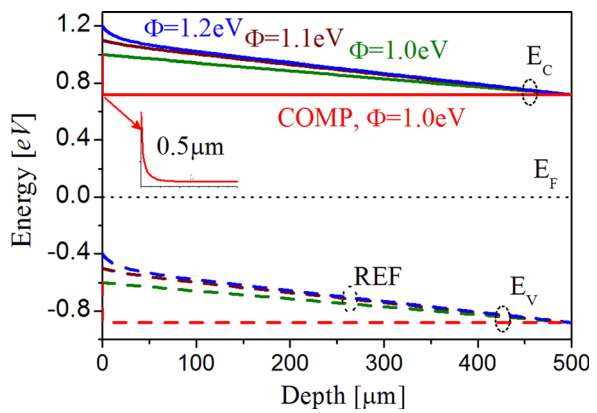

FIG. 1. Calculated energy band diagrams at TDE under Schottky contacts with various barrier potentials on high-ρ $Cd_{0.85}Zn_{0.15}Te$. Comparison of uncompensated, ν-type (REF) material ($\Phi_B = 1.0$, 1.1, and 1.2 eV), and compensated case ($\Phi_B = 1.0$ eV). The inset zooms on the compensated material in the frontmost 0.5 μm layer.

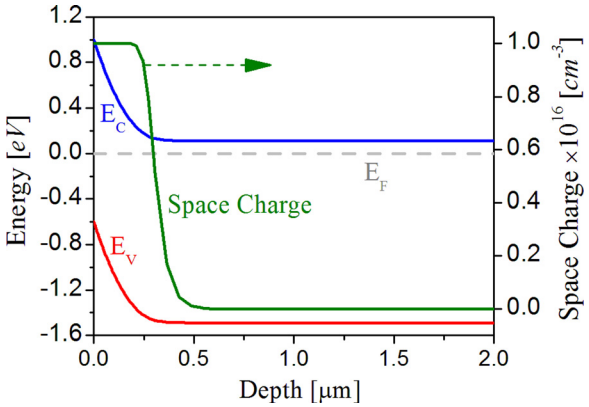

FIG. 2. Calculated energy band diagram and space charge density depth profile at TDE under Schottky contact ($\Phi_B = 1.0$ eV) on low-ρ n-type $Cd_{0.85}Zn_{0.15}Te$ ($N_D = 10^{16}\,\mathrm{cm}^{-3}$).

For comparison, similarly calculated energy band diagram and space charge density of an extrinsic case with $N_D = 10^{16}\,\mathrm{cm}^{-3}$ are shown in Fig. 2. The depletion approximation in this case is valid as indicated by the practically constant space charge profile ($\sim N_D^+$).

In the bulk of deep-donor *heavily* compensated semiconductors, the donor energy level is below the Fermi level with only a small fraction being charged ($N_{DD}^+ \ll N_{DD}$). Under a Schottky contact at TDE, the trap energy level crosses the Fermi level, thus a positive space charge region is formed near the interface with $N_{DD}^+ \approx N_{DD}$. Consequently, the energy band diagram of the compensated $Cd_{0.85}Zn_{0.15}Te$ device *at TDE* is fairly similar to the "textbook" extrinsic case with $N_D = 5 \times 10^{18}\mathrm{cm}^{-3}$. This is shown in Fig. 1 (and its inset) comparative to the REF case. It is important to note that in the compensated semiconductors at TDE the profiles are independent of the deep-donor cross-sections.

The issue of one-dimensional Schottky contacts (infinite lateral size) on an uncompensated and compensated $Cd_{0.85}Zn_{0.15}Te$ is described in more details elsewhere.[3,4]

B. Infinite Schottky contacts under reverse bias

The thermionic emission process limits the majority carrier flow from the contact into the semiconductor, while the electric field drifts them toward the back contact.

Interface carrier concentrations at TDE under 1 eV Schottky barrier are identical in low and high resistivity semiconductors, since the barrier is defined as $E_C - E_F$ at the interface (the amount of band-bending in low- and high-ρ semiconductors is different for the same barrier height).

Thus, the statement $[p]^S_{TDE} \gg [n]^S_{TDE}$ is valid also for the low-ρ ("textbook") case; however, the hole current component is absolutely negligible (unless very high generation rate exists in the depletion region). Most of the reverse bias drops on the depletion region leaving very small bulk E-field. The main current is that of thermionic emission of the electrons ($\sim$16 pA/cm^2).

1. Infinite Schottky contacts under reverse bias on non-compensated semiconductors

In the semi-intrinsic semiconductor, the space charge is very low and any reverse bias causes majority carrier *swept-out* (in fact even built-in potential is sufficient). Considerable E-filed is present throughout the bulk; therefore, the *minority* carriers generated at the back-side ohmic contact are drifted by the E-field, and become the dominant current conduction mechanism (and not the thermionic emission process, as often assumed). For n-type doping of $N_D = 6.02 \times 10^5\,cm^{-3}$ electron and hole TDE *bulk* densities are $\sim 6.13 \times 10^5$ and $\sim 1.1 \times 10^4\,cm^{-3}$, respectively. Since the back contact is defined as ideal ohmic, it maintains at the interface bulk TDE carrier concentrations (even under bias). Thus, the effective semiconductor resistivity under *reverse bias* becomes approximately $(q \times \mu_h \times [h])^{-1} \sim 10^{13}\,\Omega$cm. Due to the low space charge density throughout the bulk the E-field is practically uniform ($\approx V_{bias}/d$) as in ohmic MSM device. However, unlike in the ohmic contact case, the bulk is depleted of electrons ($n \times p \ll n_i^2$), thus thermal generation current should be considered.

2. Infinite Schottky contacts under reverse bias on compensated material

For the compensated semiconductors, the occupancy of the deep-donors under bias will be determined by the capture cross-sections and the free carrier concentrations. Figures 3(a) and 3(b) describe the charged fraction (N^+_{DD}/N_{DD}) dependence on the free electron and hole densities, respectively. Reverse bias drifts the electrons toward the back contact and holes toward the front contact, thus it tends to reduce the hole-rich region and to extend the electron depleted volume.

In case of HL traps, the occupancy of the deep donors is practically independent of $[h]$ and determined exclusively by $[e]$. The inflow of electrons from the front contact is limited by the thermionic emission over the Schottky barrier ($\sim 1.6 \times 10^{-11}$ A/cm^2). Thus, the external E-field causes the expansion of the electron depleted region under the Schottky interface (drifts the free-electron cloud). This "exposure" of deep-donors yields a positive space charge buildup under the Schottky contact (with density $N_{DD}{}^+ \sim N_{DD}$). Since the charging is inversely proportional to the free majority carrier concentration, the result resembles extrinsic uncompensated case (with high N_D). Due to the high density of charge in SCR (space charge region), it is only $\sim 0.2\,\mu$m thick, and most of the external potential develops over this frontmost layer, while the rest of the bulk is practically neutral. The *electron current* through the bulk is comprised of the thermionic emission, and comparable generation inside the SCR. The concentration of electrons in the bulk is considerable

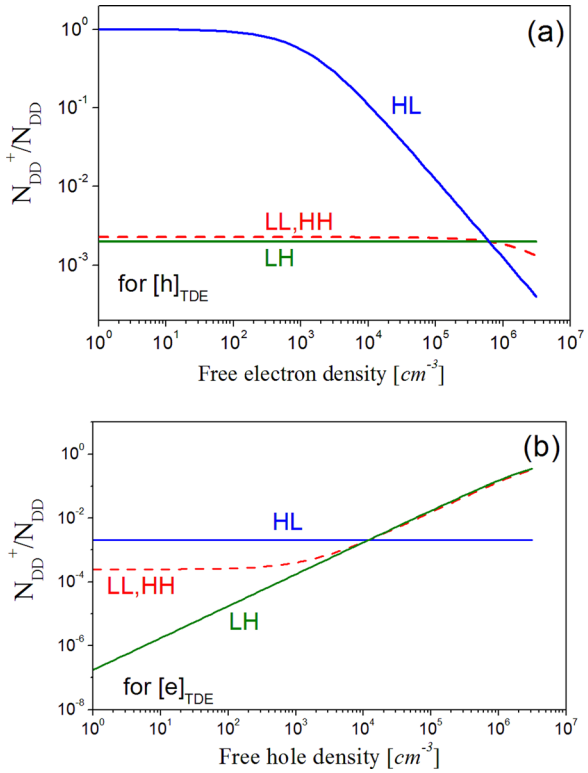

FIG. 3. Deep donor vacancy dependences on free carrier concentrations for LL, LH, HH, and HL trap sets. (a) Dependence on electron density for $[h]_{TDE}$; (b) dependence on hole density for $[e]_{TDE}$.

($\sim [e]^B_{TDE}$), but the E-field is very low. Due to the low E-field in the bulk and relatively low $[h]^B_{TDE}$ density, the influx of holes from the neutral bulk into SCR is negligible, thus most of the holes exiting through the Schottky interface are those generated in the SCR. Since the SCR expansion with bias is rather limited (due to its high density), the I-V curve exhibits sharp increase near 0 V (thermionic emission component plus initial SCR generation), followed by a slow rise.

The HH and LL sets are similar in terms of trap occupancy functions: the $N_{DD}{}^+$ charge under the Schottky contact is practically insensitive to electron *depletion*, but increases with hole accumulation above TDE concentration (in contrast to the HL case). The principal difference between the two cases lays in the high generation-recombination rate of HH material compared to LL case. For LL case, the electric field successfully sweeps the electrons out of the entire bulk, since the inflow of electrons is limited by the Schottky barrier, and electron depletion does not generate considerable SCR through varying the deep donor occupancy. The hole-rich layer shrinks under -100 V to $\sim 0.2\,\mu$m, which corresponds to SCR layer. The remaining bulk is not quite neutral due to electron depletion, but the space charge is low enough to yield a practically uniform E-field profile ($\approx V_{bias}/d$). On the other hand, in the HH set the intense generation (up to $\sim 10^{15}\,cm^{-3}s^{-1}$) increases both [h] and [e] bringing most of the bulk to neutrality ($[e] \approx [e]^B_{TDE}$, $[h] \approx [h]^B_{TDE}$). Due to the enhanced hole generation and drift toward the Schottky contact, a secondary hole-accumulated layer appears within frontmost 3–4 μm (in addition to the interface $\sim 0.2\,\mu$m layer where $[h] \gg [h]^B_{TDE}$). The secondary, thicker layer has very

light hole accumulation yielding space charge density of $\sim 5 \times 10^{15}\,\mathrm{cm}^{-3}$ (because of N_{DD}^{+} variation). This results in increased potential drop over the total SCR (over 60% of the external bias); and nearly neutral bulk with uniform E-field distribution. In LL set, the electron current contribution is limited to the thermionic emission level ($\sim 1.6 \times 10^{-11}$ A/cm^2), and the dominant current conduction mechanism is that of drifting *minority* carriers (holes). Thus, the effective resistivity is $\sim (q \times \mu_h \times [h])^{-1} \sim 10^{13}\,\Omega$cm. In HH set, the dominant current mechanism is generation in the high-space charge region; the generated holes are drifted toward the Schottky contact and exit as "hole-current"; the generated electrons are drifted toward the "neutral" bulk and eventually exit the ohmic contact as electron-current. As the external bias increases, the SCR expands consuming more potential drop, and the E-field increase in the neutral bulk region is sub-linear with the bias. Thus, the overall I-V curve is also sub-linear. In the LL case, the Schottky hole-current origins mainly from the bulk drift, whereas in the HH set most of the holes origin in the SCR generation.

In LH set, the occupancy is determined by the hole density. Under reverse bias, this case is very similar to LL, with a minor discrepancy is in the bulk hole concentration ($[e]_{LL}^{B} < [e]_{LH}^{B}$ by a few percent), which leads to a corresponding difference in currents.

3. Infinite Schottky contacts under reverse bias—impact of velocity saturation

The current-voltage (I-V) characteristics normalized to 1 cm^2 contact area are shown in Figs. 4(a) and 4(b) on logarithmic and linear scales, respectively. For semi intrinsic (REF) semiconductors, introduction of velocity saturation has no noticeable effect on the current-voltage dependence nor on the internal parameters (carrier concentrations, E-field, etc.), since the E-field throughout the device is too low to cause mobility reduction. The E-field does not reach velocity saturation threshold (up to −100 V bias), and I-V slope corresponds to bulk hole conductivity, $\sigma \cong q\mu_p [h]_{TDE}^{B}$ (the bulk is depleted of electrons, as described above). The non-dominant e-current component due to the thermionic emission does not saturate up to −100 V (the E-field under the Schottky barrier is not high enough).

In *all* compensated materials, the e-current component at the Schottky contact (thermionic emission current) saturates at a few volts bias. For constant mobility the interface electron density, $[e]^{S} \to 0$ even at low external bias, yielding a full thermionic emission current contribution. In presence of velocity saturation effect, unless $v_{Sat} \gg v_{TE}$, $[e]^{S} \not\to 0$, the saturated e-current components through the Schottky contacts are lower in all compensated devices. In HL set, the E-field in the bulk is very low thus the overall current is limited to the thermionic emission of electrons over the Schottky barrier, and SCR generation (yielding h-current through the Schottky contact). Due to the high density of charge, the SCR is narrow and has weak bias dependence. Velocity saturation reduces the saturation level of the dominant, e-current, while the h-current component remains similar. The LL and LH sets yield rather similar I-V curves. The e-current components at the Schottky

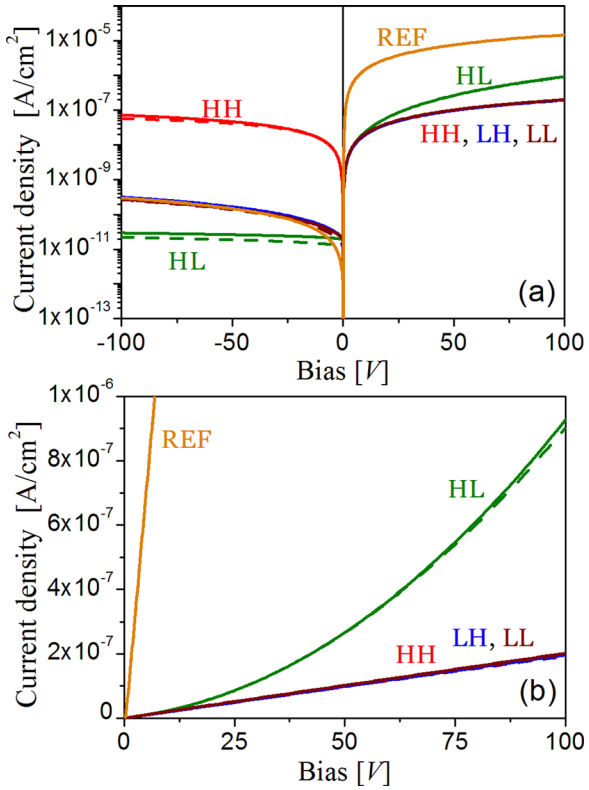

FIG. 4. Calculated Schottky contact currents, for infinite contact size on 500 μm thick bulk, normalized to 1 cm^2 area, for $\Phi_B = 1$ eV barriers on high-ρ $Cd_{0.85}Zn_{0.15}Te$ (REF, LL, LH, HL, HH sets). Solid lines represent constant mobility cases, and broken curves describe currents with velocity saturation models. Most broken lines coincide with the solid ones. (a) Logarithmic scale, (b) linear scale forward polarity.

contact saturate with and without velocity saturation effect to different values, as mentioned above. The dominant h-current components have practically linear dependence on bias and it is mostly due to drift, with a minor generation component. The HH set yields the highest currents due to dominant thermal generation, which restores near TDE carrier concentrations in most of the bulk. The I-V dependence is sub-linear since the positive space charge under the Schottky contact increases considerably with the current, drawing extra potential drop.

The LL and LH sets have lower currents compared to the HH case, and higher bulk E-field distributions than the HL case. Thus, the LL and LH materials are advantageous for detection applications, with a small advantage to LL case due to lower current.

C. Infinite Schottky contacts under forward bias

1. Infinite Schottky contacts under forward bias on non-compensated semiconductors

In an uncompensated, *extrinsic* semiconductor (low-ρ) the positive space charge of the depletion layer is mainly that of shallow donors, and $N_D^{+} \approx [e]_{TDE}^{B}$. Thus, under forward bias the majority carriers entering the depletion layer, decrease the space charge *considerably*, and reduce the energy band bending. This reduces the potential barriers for the majority carriers to exit the semiconductor (through the Schottky contact) and for the accumulated minority carriers

at the interface to flow into the bulk. With increasing forward bias, the barrier becomes negligible allowing nearly free extraction of electrons and injection of holes (limited only by Richardson interface velocity). For $\Phi_B = 1$ eV, the minority concentration at the interface, $[h]^S_{TDE} \approx 6 \times 10^8\,\mathrm{cm}^{-3}$, is much higher than $[h]^B_{TDE}$; however, it is still negligible compared the bulk majority concentration, $[e]^B_{TDE}$. Thus, even with minority carrier injection from the interface (to the limit of $[h]^B \rightarrow [h]^S_{TDE}$) the current transport is mainly performed by the majority carriers. The thermionic emission approximation of Eq. (1) is valid for *low* forward bias values. Most of the external bias develops over the junction region as long as the thermionic emission remains the limiting current component. Once the potential barrier becomes negligible, the additional bias will develop over the series bulk "resistor" and the I-V dependence becomes linear with a slope roughly proportional to $qN_D\mu_n$.

In SI, ν-type semiconductor (REF case) with a Schottky barrier of 1 eV the interface concentrations of holes and electrons are approximately $[h]^S_{TDE} \approx 6 \times 10^8$ and $[e]^S_{TDE} \approx 10\,\mathrm{cm}^{-3}$, respectively (compared to $[e]^B_{TDE} \approx 6.1 \times 10^5$ and $[h]^B_{TDE} \approx 1.1 \times 10^4\,\mathrm{cm}^{-3}$ in the bare bulk). Therefore, when positive bias is applied to such device the minority carriers injected from the Schottky interface into the bulk dramatically modify its resistivity. The hole density in the bulk can practically reach the interface value even at relatively low bias. The resulting I-V curve is virtually linear corresponding to *effective* bulk resistivity $\sim (q \times \mu_h \times 6 \times 10^8)^{-1} \approx 1.3 \times 10^8\,\Omega$cm, as shown by the REF curve in Fig. 4(b). Therefore, in SI material the minority carriers conduct most of the current *in both polarities*, and the thermionic emission contribution expressed by Eq. (1) *cannot* be used for total current estimates. It should be noted that for barriers >1.1 eV hole injection leads to space charge limited current (SCLC) conditions.[3]

2. Infinite Schottky contacts under forward bias on compensated semiconductors

The characteristics of Schottky contacts simulated on deep-trap compensated materials are very different from the characteristics of such contacts on semi-intrinsic and extrinsic semiconductors. Both, macroscopic properties (such as the overall, externally "measured" currents) and microscopic behavior (such as E-field distribution inside the semiconductor), greatly depend on the deep donors' cross-sections. The main difference is in the origin and density of the space charge forming the potential barrier. Whereas, in an extrinsic "textbook" case described above, under forward bias the "shift" of the "majority carriers cloud" towards the junction neutralizes the dopant ions, reducing the potential barrier, in heavily compensated materials the SCR density, $\sim N^+_{DD}$, is *much* higher than $[e]^B_{TDE}$; therefore, the *net charge* of the free electrons pulled toward the Schottky contact falls short to compensate for N^+_{DD}. Everything depends on the occupancy dependences of the deep traps.

In LH, LL, and HH sets, the occupancy is independent (LH) or weakly dependent (LL, HH) on $[e]$, but strongly dependent on $[h]$. Since under the contact $[h]$ is high ($>10^7\,\mathrm{cm}^{-3}$), $N^+_{DD} \approx N_{DD}$, and the forward bias has limited impact on the potential barrier reduction (in spite of the increase in $[e]$ near the interface). Under positive bias, in presence of such SCR, the Schottky barrier creates a valley in the conduction band and a hump in the valence band (at some distance from the interface).

The valence energy band evolution of LH material under increasing forward bias is shown in Fig. 5. The hump in the valence energy band hinders the influx of holes from the interface into the bulk (generating a drift component opposite to the diffusion). It is interesting to note that with increasing forward bias the hump is not easily reduced (as in low-ρ case), meaning that most of the external bias increase develops over the bulk rather than the junction region. There is a "negative feedback" mechanism reducing variations of SCR with bias: reduction of hump increases hole injection, leading to the expansion of hole-rich layer, which leads to N^+_{DD} increase (since $[N^+_{DD}/N_{DD}] \propto [h]$) $\rightarrow$ hump increase. The interface SCR is dense, but very thin, therefore the potential drop over the barrier region is negligible and most of the potential drops over the bulk. The electrons *drift* from the nearly neutral bulk *accumulating* in the conduction band valley; at the bottom of the valley, the E-field vector reaches zero and *changes direction*; thus, the accumulated electrons *diffuse* from the valley minimum point toward the interface (opposite to the local E-field direction). With increasing bias the minimum point of the valley slightly rises and moves closer to the Schottky interface; thus, the concentration of the accumulated electrons and the diffusion current density *increase*.

In LL material N^+_{DD} decreases with increasing $[e]$ above $[e]_{\mathrm{TDE}}$, and with decreasing $[h]$ below $[h]_{\mathrm{TDE}}$ (as seen in Fig. 3). As forward bias is applied, the electrons begin accumulating in the conduction band valley (similar to the LH set). However, increasing electron concentration *reduces* the local space charge density, which reduces the valley depth. The corresponding reduction of the valence band hump promotes hole-diffusion, which, in turn, widens the SCR ($N^+_{DD} \propto [h]$). The potential hump becomes smaller in magnitude, but significantly wider, as seen in Fig. 6.

The nearly overlapping, linear I-V curves of sets LL and LH in Fig. 4(b) manifest bulk electron conduction with $[e] \approx [e]^B_{TDE}$ as the current limiting step.

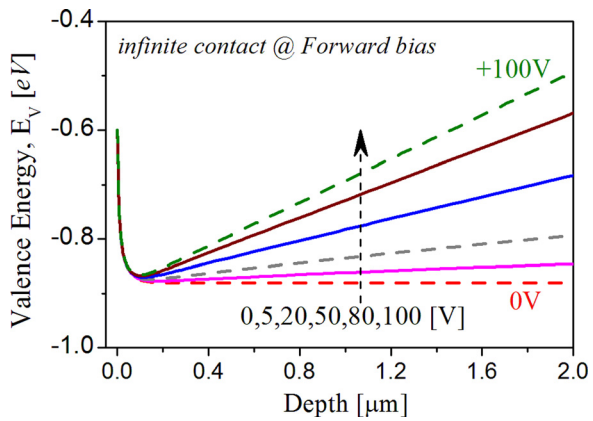

FIG. 5. Calculated valence energy band diagram under infinite Schottky contact ($\Phi_B = 1$ eV) on compensated (LH set) material. Zoom on frontmost 2 μm layer, with applied forward bias potentials between 0 and 100 V.

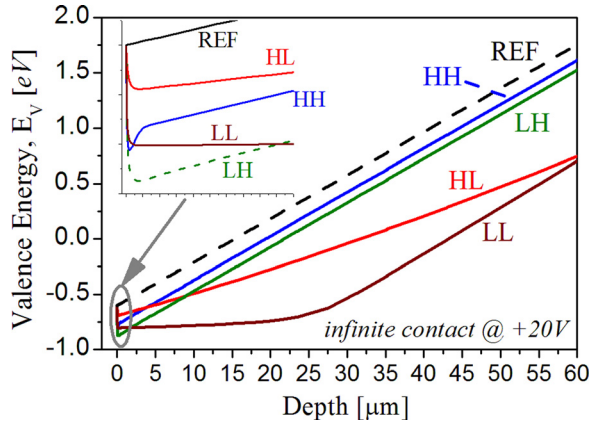

FIG. 6. Calculated valence energy band diagram under infinite Schottky contact (Φ_B= 1 eV) on all compensated and REF materials at +20 V bias. Calculated bulk thickness is 500 μm, the figure shows the foremost 60 μm under the Schottky contact. The inset further zooms on frontmost layer.

Although the I-V curve of HH device nearly coincide with LL, and LH sets, there is an important distinction in the current flow mechanism between low G-R (generation-recombination) materials (LL, LH) and high G-R case (HH). In LL and LH materials, the electrons *accumulate* in the conduction band valley, which increases the *electron-diffusion* current toward the interface (and their thermionic emission). In the HH case, the accumulation of electrons under the contact is practically cancelled out by the high recombination rate. Thus, electron drift current from the bulk *is converted through recombination into hole current* diffusing from the Schottky interface. In all three cases (LL, LH, and HH), the electron current is dominant and the current limiting step is drift through the bulk, whereas the potential drop over the barrier is small.

Exception is the HL set, where electron density above $10^3\,cm^{-3}$ reduces the charged fraction of the deep-donors considerably (see Fig. 3(a)), which lowers the "hump" in the valence energy band. The holes injected into the bulk over the lowered hump *do not affect the occupancy* of the deep-donors. The bias dependent increase of [*h*] in the bulk causes super-linear I-V curve, and the dominant current component switches from e-current to h-current at very low bias.

3. Infinite Schottky contacts under forward bias—impact of velocity saturation

The introduction of velocity saturation has negligible effect in infinite contacts under forward bias in compensated and SI semiconductors since the bulk E-field is well below the critical value.

D. Scaling Schottky contacts under reverse bias

In absence of shunting leakage channels and given low G-R rate in low-ρ material, the reverse Schottky current is dominated by thermionic emission (as shown for infinite contact case above). The thermionic current density saturates as $[e]^S \rightarrow 0$. Thus, for low-ρ case the contact saturation currents scale strictly with the contact area (r^2) for all radii down to 10 nm. The bias required for the saturation reduces with decreasing contact size (due to increasing E-filed).

In high-ρ materials, the reverse currents in infinite Schottky contacts vary in magnitude and conductivity mechanisms for various material types. Yet, for each material the currents scale with the contact *area*, as long as the radius remains above a critical value, r_{cr}. This is shown in Fig. 7(a) presenting the total currents at −100 V bias versus contact radii. The log-log scale representation yields linear fits with slopes of ~2, for all material types (indicating r^2 dependence). The value of r_{cr} appears to be not only a function of geometry but also of material type. This is exhibited in Fig. 7(b) focusing on the intermediate-small contact radii current-scaling. For uncompensated (REF), LL, and LH materials, r_{cr} is comparable to the bulk thickness (500 μm); however, for HH and HL materials the value or r_{cr} extends down to 10 μm. In contacts below critical radii ($r < r_{cr}$), reverse currents scale with the contact radius (or periphery), in all materials, except HL case. These are macroscopic observations on total contact currents, and in order to explain them one has to look deeper into devices anatomy.

For low space charge case, such as SI semiconductor, the E-field distribution under Schottky contact is very similar to the ohmic contact instance. Namely, for infinite contacts the E-field is practically uniform throughout the bulk; for point contact the E-field decreases with distance as d^{-2}; contacts with $r \gg t_{Bulk}$ (radius ≫ bulk thickness) are similar to the infinite contact, except for the edge region; in "small"

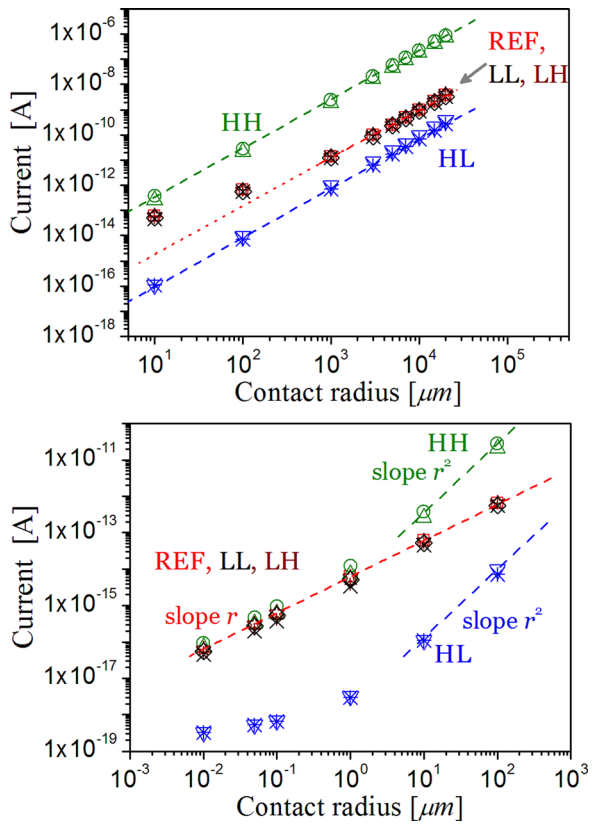

FIG. 7. Log-Log plot of the total contact currents versus contact radii at −100 V bias. Schottky contact (Φ_B = 1 eV) on high-ρ $Cd_{0.85}Zn_{0.15}Te$ (REF, LL, LH, HL, HH sets). (a) Focus on large contacts; (b) focus on intermediate-small contacts.

contacts with $r < t_{Bulk}$ the electric field remains nearly constant and perpendicular to the interface down to ~0.5 r depth (except the edge area), followed by radial dispersion of the E-field lines. In such "small" contacts, the intensity of the electric field in the "plateau" region (0 to ~0.5 r from the interface) is inversely proportional to the contact radius, as seen in Fig. 8.

The *radial* non-uniformity of the E-field intensity, manifested in all finite contacts (ohmic and Schottky), may affect the drift current component (unless velocity saturation limit is reached). Deeper insight on the impact of edge-effect on the overall contact current is brought later. The following discussion focuses on the central region of the contact (J_{Center}).

Under reverse bias, the contact region is depleted of electrons and the current at the Schottky interface is dominantly conducted by holes. The current density is approximately given by $J \approx qpv_h$. In the absence of significant diffusion component, the *effective* velocity approaches *drift* velocity (for constant mobility $v_d = \mu E$). Free hole density profiles under the centers of 100 nm, 1 μm, and 10 μm radii contacts are presented in Fig. 8, combined with the corresponding E-field profiles. Clearly, the hole-rich interface layer is very narrow compared to the E-field plateau region (noting the logarithmic distance scale). Namely, most of the high-plateau E-field region under the Schottky has a *constant* hole density ($\sim[h]^B_{TDE}$), and only a thin layer is hole-rich. Although in the hole rich region the E-field remains constant (and high) the current density does not increase with $[h]$, because it is no longer given by σE, due to a significant gradient in hole density, causing *opposite* diffusion current. Thus, for manual calculations the easiest deduction of the contact current is not at the interface, but from the region combining constant E-field *and* constant $[h]$, where the drift velocity approximation is valid on one hand and the lateral current component is negligible on the other. The current is roughly proportional to the contact area, times the E-field plateau value (excluding the edge-effect), times $[h]^B_{TDE}$. The E-field plateau value in small contacts is *inversely proportional* to the contact radius. Thus, I_{Center} ($=J_{\mathrm{Center}} \times$ Area) in small contacts and in absence of a significant space charge is proportional to the *contact radius*, rather than area (as in large contacts).

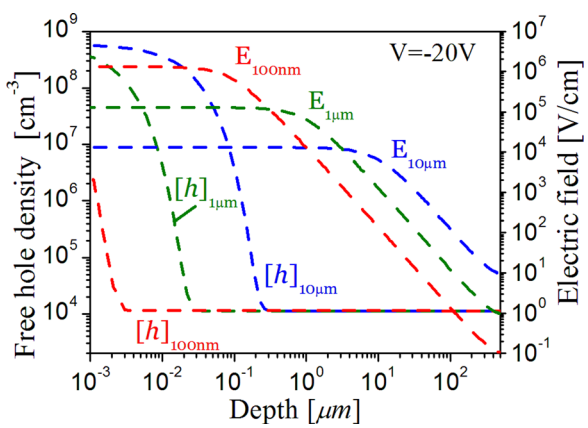

FIG. 8. Depth profiles of electric field and hole density profiles under centers of 100 nm, 1 μm, and 10 μm contact radii. Calculated at −20 V bias for 1 eV barrier Schottky device on REF $Cd_{0.85}Zn_{0.15}Te$.

Under Schottky contacts on heavily compensated semiconductors, high density space charge develops, limiting the E-field propagation toward the back contact (even in infinite contacts). In LL and LH sets, the high SCR is limited to a few nm layer (where $[h] \gg [h]^B_{TDE}$ since $N^+_{DD} \propto [h]$), thus the potential drop over the SCR is negligible. The free carrier concentrations and the E-field profiles are similar to the REF case. The main difference in the compensated materials is the increase of E-field in the high SCR region (on top of the plateau of the REF case). However, this E-field step is only a few nm thick and does not affect the following E-field plateau value. Thus, the currents of Schottky contacts on REF, LL, and LH materials are similar, and they scale similarly with radius.

In large and infinite contacts on HH material, the currents are much higher than on other types, as discussed above. There are two interesting observations with decreasing contact size: the currents scale with radius down to ~10 μm (compared to ~500 μm in LL, LH, and REF cases); for small radii the HH currents practically coincide with LL, LH, and REF currents. Why? In HH set devices considerable net generation occurs under reverse bias, since $np < n_i^2$, raising the [e] and [h] to near TDE values in most of the bulk. Only the frontmost layer is depleted of electrons and has $[h] > [h]^B_{TDE}$ which results in increased SCR density ($N_{DD}{}^+$) and a corresponding E-field intensification. In larger contacts, the main current component is due to electron-hole generation in that high E-filed region, as discussed in the infinite case. Thus, the total current is proportional to the high-E-field *volume* (which is depleted of electrons, maintaining $np < n_i^2$). For large (and infinite) contacts the *depth* of the high-E-field layer is ~3 μm, and therefore the volume is proportional to the area (current scaling with r^2). When the radius is downscaled *to a few microns*, the space charge region becomes spherical, and the gradient of E-filed increases. While its interface value rises, in the rest of the "generating volume" ($np < n_i^2$) the E-field decreases and becomes insufficient to extract the carriers efficiently. Thus, the generation current component decreases. The main mechanism becomes the same as in LL case and the two currents equalize.

The deep donor occupancy in HL case is insensitive to $[h]$, but very sensitive to $[e]$. Due to electron depletion under the contact $N_{DD}{}^+ \approx N_{DD} = 5 \times 10^{18}$ cm^3. Most of the external bias drops over the SCR, and this configuration yields the lowest current. The E-field under the contact center is higher than in other materials and does not scale with 1/r as in other cases. In fact it is nearly independent of the contact radius (down to 50 nm radius). In the larger contacts, the current comprises mostly of SCR carrier recombination and thermionic emission of electrons over the Schottky barrier. Due to the high E-field, the SCR layer is practically depleted of holes, but their concentration increases for radii below 100 nm. The later combined with increasing E-field makes hole-current dominant and weakly dependent on the radius. Namely, since *both*, E-field and $[h]^{SCR}$ increase with downscaling below 100 nm, the *current density* increases nearly with r^2.

Velocity saturation impact on the current in uncompensated material is negligible. In compensated materials, the impact is as follows. In large contacts on LL and LH materials, the introduction of velocity saturation mainly reduces the e-current component (as in infinite contacts), with negligible effect of scaling; in HH set the increase of [h] caused by mobility reduction near the contact causes corresponding SCR and E-field buildup, which in turn reduces the bulk E-field, leading to current decrease (up to 50% at −100 V); in HL set velocity saturation effect reduces the e-current saturation level (as described for infinite contacts). The current changes are limited and the scaling rules for *all* materials are similar to the constant mobility case as shown in Figs. 7(a) and 7(b).

In general, the electric field under *small* contacts is very high and without velocity saturation effect the hole drift velocity, v_{dh}, can easily reach above 10^8 cm/s. Thus, one could expect a drastic current decrease when v_{dh} is limited to $v_{dh,SAT} = 10^7$ cm/s. However, the reverse currents are not radically reduced by the velocity saturation effect, due to considerable "compensating" hole accumulation in the region (yielding $J \gg [h]^B_{TDE} \times v_{dh,SAT}$ near the contact interface). The effect is similar to the one described in ohmic contacts,[35] where holes drifting from a larger bulk volume into a smaller contact region at constant velocity pile-up under the contact.

The "edge-effect" is manifested by increased E-field around the edges. The thermionic emission of metal electrons over the Schottky barrier is not a function of the E-field intensity in the semiconductor as long as there is no barrier lowering. Thus, in the low resistivity semiconductor (with valid thermionic-emission approximation), there is no observable impact on the total contact current under reverse bias. However, in high-ρ semiconductors the role of minority carriers is pronounced (often even dominant), therefore radial [h] distribution under the contact plays a significant role. Figure 9 exhibits the dependence of J_Y (*perpendicular* to the interface component of the current density) on radial distance from the contact center. The curves correspond to uncompensated, SI material without velocity saturation,

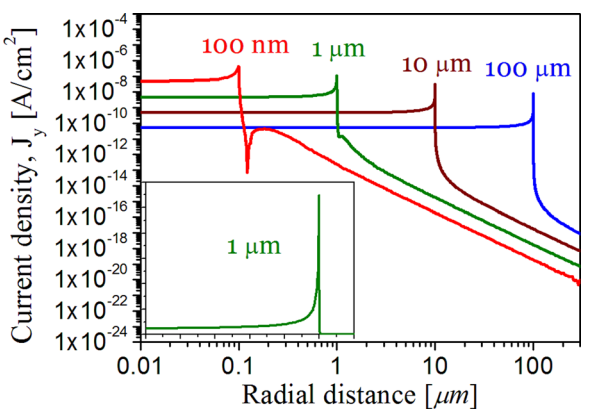

FIG. 9. Lateral profiles of the normal-to-contact component of the current density (J_Y) under centers of 100 nm, 1 μm, 10 μm, and 100 μm contact radii. Calculated at −5 V bias for 1 eV barrier Schottky device on REF $Cd_{0.85}Zn_{0.15}Te$. Inset exhibits the data for 1 μm radius contact on linear scale.

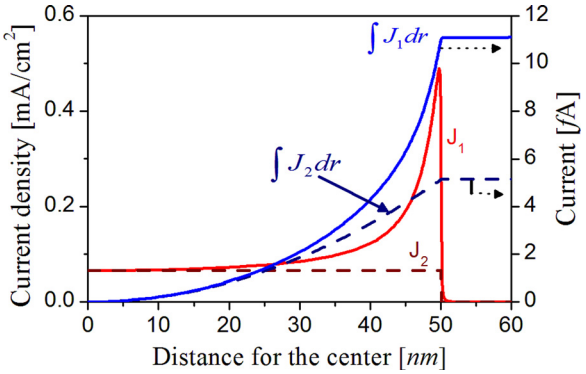

FIG. 10. Radial distribution of the current density component J_Y, and its Riemann integral function ($\int_0^x J_Y dr$) for a 50 nm radius contact on REF $Cd_{0.85}Zn_{0.15}Te$. Curve J_1 and its definite integral represent the detailed calculation results (accounting for the "edge effect"), while curves J_2 and its integral assumes uniform current density (center value).

and were calculated for −5 V bias near the interface for contact radii of 100 nm, 1 μm, 10 μm, and 100 μm. The inset shows J_Y for 1 μm contact radius on *linear scale*. These current density distributions follow the E_Y-field profiles (the E-field component perpendicular to the Schottky interface). Numerical radial integration of J_Y current density indicates that the edge current peak increases the total contact current by a factor ~2 (compared to uniform current density distribution with $J = J_{Center}$). Example of such calculations with r = 50 nm contact, biased at −5 V, for constant current density assumption ($J = J_{Center}$), and for "real" calculated current density distribution is shown in Fig. 10.

The impact factor of the edge effect on the total contact current changes roughly between 1 and 2 depending on the contact size and material type. However, for each material this impact factor changes *gradually*, e.g., for SI (REF) set the factor varies from 1 to 2, while the radius changes by 2 orders of magnitude (area changes by 4 orders of magnitude). Therefore, the edge effect impact on the current is not negligible for each contact; however, it has a negligible impact on contact-current *scaling* (Figs. 7(a) and 7(b)).

E. Scaling Schottky contacts under forward bias

For large contacts the E-field depth distribution and the energy band profiles are independent of the contact radii. Therefore, for each material the currents scale linearly with the contact area (r^2). However, as the contacts are shrunk the scaling becomes complex and bias dependent.

In low-ρ material the current scales with area for low bias voltages, while thermionic emission limits the current. As the bias increases the potential barrier disappears, and electrons accumulate at the interface facilitating further current increase in spite of limited Richardson velocity ($v_{h,RC}$). The current scaling changes from r^2 to r dependent.

In uncompensated material, the potential barrier is rapidly cancelled out under forward bias. Thus, the "interface holes" are injected into the bulk not by diffusion over the potential hump (as in compensated or low-ρ materials), but rather by E-field. In large contacts up to +100 V bias, the interface hole

density, $[h]^S$, does not change significantly with bias (or contact radius), and $[h]^B \rightarrow [h]^S \approx [h]^S_{TDE}$. Therefore, the I-V curves correspond to ohmic contacts on *p-type* $Cd_{0.85}Zn_{0.15}Te$ with $N_A \sim 6 \times 10^8\,cm^{-3}$. With reducing contact size and correspondingly increasing E-field intensity at the interface, Richardson velocity becomes a limiting factor, reducing $[h]^S$ drastically. The hole-current density *saturates* according to Eq. (2) at $I_{h,MAX} = Aqv_{TE,h}[h]^S_{TDE}$ [A], as $[h]^S \rightarrow 0$ (where $v_{TE,h}$ is the hole Richardson velocity, A is the contact area, and q is the electron charge). The dominant current mechanism of large contacts saturates in smaller contacts (and/or high forward bias voltages), leaving the lead to electron bulk current (similar to ohmic contacts on n-type semiconductor with $N_D \sim 6.1 \times 10^5\,cm^{-3}$). Electrons accumulate at the interface to facilitate the current increase according to Eq. (2).

Namely, for a given contact size the "current mechanism inversion" occurs at a corresponding bias, alternatively if we down-scale a contact kept at constant forward potential, a similar transition occurs. Saturation h-current *density* is constant, thus its current component is proportional to r^2, while electron current increases as in ohmic contacts (proportional to r). Thus, only when saturation h-current becomes negligible, the current will scale with r.

Equivalently, under forward bias *all* contacts having high E-field density exhibit current "step" (saturation of hole-current contribution). This high field could be due to small contact size, or high SCR density, as in compensated materials.

Under forward biased Schottky contacts on compensated materials, the energy bands bend upwards creating a minimum point (dE/dx = 0)—namely, conduction band valley and valence band bump, as explained for infinite contacts. In all compensated materials for large contacts currents scale with r^2 as in reverse bias case (the energy band bending is not r dependent). The LL, HH, and LH sets exhibit linear I-V curves, whereas HL curves are super-linear, but all scale with r^2. As the contact size is further reduced the SCR screening geometry changes and the band bending changes accordingly, as shown in Fig. 11 for LL and LH materials at +20 V. The reduction of the hump height and its shift toward the interface is common to all materials. In LL cases, the minimum point fades with increasing forward bias and contact size reduction, enabling interface accumulation of electrons, and hole drift from the interface. Beyond that bias the electrons drift all the way to the interface without any potential barrier as in ohmic contact case. Therefore, for *small* contacts (and/or high forward bias potentials) the dominant electron-current scales as I ∝ r (*similar to the ohmic contacts*[35]). For intermediate size contacts (μm scale) and/or low bias, the interface hole-concentration, $[h]^S$, changes with contacts radius and bias (not saturated on one hand and nonlinear I-V dependence on the other). At the same time, the electron-current is not yet dominant, therefore there is no obvious current scaling. In LH case the hump is reduced with decreasing r. The resulting current scaling is complex and bias dependent. In HH case the hump fades only for radii below 100 nm and only at high bias. Thus, it is similar to LH in terms of scaling. In HL case the accumulation of electrons reduces the deep donor occupancy, which reduces the SCR and the hump. Thus, the current scaling in small contacts is as for REF and LL materials.

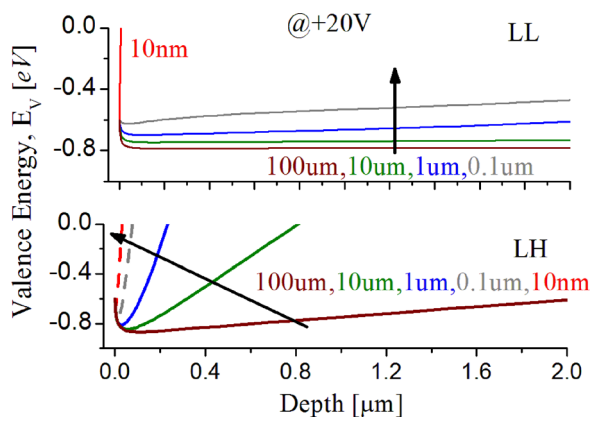

FIG. 11. Depth profiles of the valence energy band under Schottky contacts ($\Phi_B = 1$ eV) on LL and LH materials. The calculations performed at +20 V bias for 10 nm, 100 nm, 1 μm, 10 μm, and 100 μm contact radii.

Introduction of velocity saturation model into scaling has the following effect. The evacuation of holes from the interface is poorer due to limited velocity, thus unless $v_{h,sat} \gg v_{TE,h}$, the interface density, $[h]^S \not\rightarrow 0$ with increasing bias. This reduces the hole saturation current. The volume of the electron accumulation region increases compensating for the mobility reduction in high E-filed zone. The overall I-V curves in REF material remain very similar with and without the velocity saturation effect for small contacts (when e-current dominates); for contact radii $100\,\mu m < r < 1\,\mu m$, the difference is noticeable because the dominant h-current is decreased ($v_h \sim v_{TE,h}$); in contacts with $r > 100\,\mu m$ the interface hole velocity is well below $v_{h,sat}$ or $v_{TE,h}$ and the velocity saturation effect is not pronounced.

Somewhat surprisingly, the introduction of velocity saturation effect *increases* the currents in LL case for $r < 10\,\mu m$. Under forward bias, velocity saturation enhances the electron accumulation under the Schottky contact (similar to the ohmic case described in Ref. 35). The *enhanced* growth of [e] causes enhanced reduction in N_{DD}^+ under the contact, which amplifies the super-linear I-V dependence described for infinite contacts (current density increases → increase in $[e]^S$ → reduction of N_{DD}^+ → decrease of conduction band valley → further increase in $[e]^S$ → the I-V curves are super-linear). However, as N_{DD}^+ decreases below N_A the space charge under the Schottky contact becomes $\sim 10^{16}\,cm^{-3}$. With further increasing bias this space charge region extends drawing considerable potential drop, as a result the current tends to saturate. In HH case, the mobility reduction of electrons drifting toward the contact is not compensated by additional electron accumulation (as in LL case) due to the effective recombination. In fact, the inflow of electrons from the bulk decreases and the conduction band valley increases. As a result, the currents decrease considerably in presence of velocity saturation. The HL case is rather similar to the LL: velocity saturation enhances the h-current at certain bias range above the constant velocity case, but then the current becomes sub-linear, while in the constant mobility case current continues to increase.

For HL case, the conduction band valley cancels out at lower bias (compared to LL), thus the current enhancement-saturation is observed even in large contacts ($r = 10\,\mu m$).

IV. SUMMARY

The impact of contact scaling on currents, electric field profiles, and free carrier densities was analyzed for Schottky contacts. The emphases were made on comparison of high- and low-resistivity semiconductors on one hand and on compensated and uncompensated semiconductors (SI, ν-type $Cd_{0.85}Zn_{0.15}Te$, $\rho \sim 10^{10}$ Ωcm), on the other. The investigated bias range extends to high values accounting for detector operation conditions. Energy band structures under forward and reverse bias voltages were studied and current mechanisms analyzed.

For low-ρ semiconductor ("textbook case") the absence of shunting leakage channels and with low generation-recombination rates it was found that under reverse bias the current scales with contact area (with r^2). The same is true for low forward bias, as long as the thermionic emission is limiting the overall current transport. For higher forward bias, the barrier levels-off enabling nearly free electron flow from the semiconductor into the Schottky contact, and injection of holes from the Schottky interface into the bulk (the limiting factor is Richardson interface velocity). Thus, in small contacts at high forward bias voltages the currents scale, as in ohmic contacts, with contact *perimeter*.

In high resistivity semiconductors, the current mechanisms and magnitudes differ considerably for various material types. However, for large contacts it was found that for each material type the currents scale with contact area (r^2), for both, forward and reverse bias.

For Schottky devices with $r_C < t_{Bulk}$ on high-ρ semiconductors, the scaling rules vary. In uncompensated (REF) $Cd_{0.85}Zn_{0.15}Te$ the E-field distribution is similar to the ohmic case for *both* polarities, yet the currents scale with r_C (as in ohmic contacts) only under reverse bias, with and without velocity saturation effect. Under forward bias, the hole-current saturates (due to finite Richardson velocity as $[h]^S \to 0$), and electron-current becomes dominant. The hole saturation current is independent on E-field and thus proportional to r^2, while the electron current (as in ohmic contacts) is proportional to r, therefore the total current scaling is mixed.

In LL, HH, and LH compensated semiconductors, the currents under reverse bias scale with area for radii above r_{cr}, and with perimeter below r_{cr}. The critical radius for LL, and LH is the same as for REF material ($\sim t_{Bulk}$), while for HH material it is a few micrometers. In HL material the scaling with r^2 extends as in HH set, down to a few micrometer radii, with no neat scaling below r_{cr}. Introduction of velocity saturation effect has small to negligible current reduction under reverse bias (further increasing accumulation of holes under the contact). Under forward bias in LL and HL cases, the extra accumulation of electrons due to velocity saturation reduces the space charge density. As a result the current with velocity saturation grows above the constant mobility case up to a certain bias, after which SCR is constant and the current tends to saturate, while the current of the constant mobility case keeps increasing.

ACKNOWLEDGMENTS

This research was supported by the Israel Science Foundation (Grant No. 322/14). The study was carried out within the framework of RD-50 collaboration at CERN.

[1]S. M. Sze, *Physics of Semiconductor Devices*, 2nd ed. (Wiley, New York, 1981).
[2]E. H. Rhoderick and R. H. Williams, *Metal-semiconductor Contacts*, 2nd ed. (Clarendon Press, Oxford; Oxford University Press, New York, 1988).
[3]A. Ruzin, "Simulation of Schottky and ohmic contacts on CdTe," J. Appl. Phys. **109**, 014509 (2011).
[4]A. Ruzin, "Simulation of metal-semiconductor-metal devices on heavily compensated $Cd_{0.9}Zn_{0.1}Te$," J. Appl. Phys. **112**, 104501 (2012).
[5]V. Palankovski and R. Quay, *Analysis and Simulation of Heterostructure Devices* (Springer, Wien, 2004).
[6]C. Y. Wu, "Interfacial layer-thermionic-diffusion theory for the Schottky-barrier diode," J. Appl. Phys. **53**, 5947–5950 (1982).
[7]A. E. Bolotnikov, S. E. Boggs, C. M. H. Chen, W. R. Cook, F. A. Harrison, and S. M. Schindler, "Properties of Pt Schottky type contacts on high-resistivity CdZnTe detectors," in *Nuclear Instruments & Methods in Physics Research Section a-Accelerators Spectrometers Detectors and Associated Equipment* (2002), vol. 482, pp. 395–407.
[8]P. Cheuvart, U. Elhanani, D. Schneider, and R. Triboulet, "CdTe and CdZnTe crystal-growth by horizontal Bridgman technique," J. Crystal Growth **101**, 270–274 (1990).
[9]F. P. Doty, J. F. Butler, J. F. Schetzina, and K. A. Bowers, "Properties of CdZnTe crystals grown by a high-pressure Bridgman method," J. Vac. Sci. Technol., B **10**, 1418–1422 (1992).
[10]K. B. Parnham, "Recent progress in $Cd_{1-x}Zn_xTe$ radiation detectors," Nucl. Instrum. Methods Phys. Res., Sect. A **377**, 487–491 (1996).
[11]O. A. Matveev, N. K. Zelenina, A. I. Terent'ev, A. A. Tomasov, and V. N. Gus'kov, "Conductivity compensation in CdZnTe: Cl crystals with variable zinc content," Tech. Phys. Lett. **33**, 358–360 (2007).
[12]P. F. Yu, W. Q. Jie, and T. Wang, "Effect of Te atmosphere annealing on the properties of CdZnTe single crystals," Nucl. Instrum. Methods Phys. Res., Sect. A **643**, 53–56 (2011).
[13]T. Sato, S. Kasai, and H. Hasegawa, "Current transport and capacitance—voltage characteristics of GaAs and InP nanometer-sized Schottky contacts formed by in situ electrochemical process," Appl. Surf. Sci. **175–176**, 181–186 (2001).
[14]T. Sato, S. Kasai, and H. Hasegawa, "Electrical properties of nanometer-sized Schottky contacts for gate control of III-V single electron devices and quantum devices," Jpn. J. Appl. Phys., Part 1 **40**, 2021–2025 (2001).
[15]G. D. J. Smit, S. Rogge, and T. M. Klapwijk, "Enhanced tunneling across nanometer-scale metal-semiconductor interfaces," Appl. Phys. Lett. **80**, 2568–2570 (2002).
[16]G. D. J. Smit, S. Rogge, and T. M. Klapwijk, "Scaling of nano-Schottky-diodes," Appl. Phys. Lett. **81**, 3852–3854 (2002).
[17]J. Osvald, "Intersecting behaviour of nanoscale Schottky diodes I–V curves," Solid State Commun. **138**, 39–42 (2006).
[18]F. Giannazzo, F. Roccaforte, V. Raineri, and S. F. Liotta, "Transport localization in heterogeneous Schottky barriers of quantum-defined metal films," Europhys. Lett. **74**, 686–692 (2006).
[19]M. A. Yeganeh, R. K. Mamedov, and S. Rahmatallahpur, "Studying of barrier height and ideality factor relation in the nano sized Au-n type Si Schottky diodes," Superlattices Microstruct. **50**, 59–68 (2011).
[20]A. Ruzin, "Simulating downscaling of ohmic contacts on wide-bandgap low-resistivity semiconductors," IEEE Trans. Electron Devices **59**, 1668–1671 (2012).
[21]A. Ruzin, O. Sinkevich, G. Cohen-Taguri, and I. Goldfarb, "Anomalous behavior of epitaxial indium nano-contacts on cadmium-zinc-telluride," Appl. Phys. Lett. **101**, 132108 (2012).
[22]P. A. D. S. T. ISE-TCAD, Synopsys http://www.synopsys.com.
[23]D. T. F. Marple, "Effective electron mass in CdTe," Phys. Rev. **129**, 2466–2470 (1963).
[24]B. Segall, M. R. Lorenz, and R. E. Halsted, "Electrical properties of n-type CdTe," Phys. Rev. **129**, 2471–2481 (1963).
[25]A. L. Mears and R. A. Stradling, "Cyclotron resonance and cross-modulation with n-type CdTe at 1 mm and 2 mm wavelength," Solid State Commun. **7**, 1267–1269 (1969).

[26]L. S. Dang, G. Neu, and R. Romestain, "Optical detection of cyclotron resonance of electron and holes in CdTe," Solid State Commun. **44**, 1187–1190 (1982).
[27]*CdTe and Related Compounds; Physics, Defects, Hetero- and Nanostructures, Crystal Growth, Surfaces and Applications*, edited by R. T. A. P. Siffert (Elsevier Ltd., 2009), p. 296.
[28]C. Jacoboni and L. Reggiani, "High field transport in CdTe at 300 degrees K," Phys. Lett. A **33**, 333 (1970).
[29]C. Canali, M. Martini, G. Ottavian, and K. R. Zanio, "Transport properties of CdTe," Phys. Rev. B **4**, 422 (1971).
[30]B. K. Ridley and T. B. Watkins, "The possibility of negative resistance effects in semiconductors," *Proceedings of the Physical Society* (1961), vol. 78.
[31]S. Selberherr, *Analysis and Simulation of Semiconductor Devices* (Springer-Verlag, Wien-New Cork, 1984).
[32]G. Ottaviani, C. Canali, C. Jacoboni, A. Alberigi, and K. Zanio, "Hole mobility and Poole-Frenkel effect in CdTe," J. Appl. Phys. **44**, 360–371 (1973).
[33]D. M. Caughey and R. E. Thomas, "Carrier mobilities in silicon empirically related to doping and field," *Proceedings of the Institute of Electrical and Electronics Engineers* (1967), vol. 55, p. 2192.
[34]C. Canali, G. Majni, R. Minder, and G. Ottaviani, "Electron and hole drift velocity-measurements in silicon and their empirical relation to electric-field and temperature," IEEE Trans. Electron Devices **22**, 1045–1047 (1975).
[35]A. Ruzin, "Scaling effects in ohmic contacts on semiconductors," J. Appl. Phys. **117**, 164502 (2015).